Journal of Polymers and the Environment (2021) 29:3185–3198
https://doi.org/10.1007/s10924-021-02111-8

ORIGINAL PAPER

Removal of Methylene Blue Dye from Aqueous Solution using PDADMAC Modified ZSM-5 Zeolite as a Novel Adsorbent

Sabarish Radoor[1] · Jasila Karayil[2] · Aswathy Jayakumar[1] · Jyotishkumar Parameswaranpillai[1] · Suchart Siengchin[1]

Accepted: 3 March 2021 / Published online: 11 March 2021

Abstract

In the present work, we modified ZSM-5 zeolite using a bio polymer poly (diallyl dimethyl ammonium chloride) and employed it for the removal of cationic dye, methylene blue from aqueous solution. The chemical and physical properties of the modified ZSM-5 zeolite were investigated using XRD, FTIR, SEM, TEM, nitrogen adsorption, TGA and ^{27}Al NMR. Modified ZSM-5 zeolite possesses high surface area and pore diameter which was confirmed from SEM, TEM and nitrogen adsorption analysis. Adsorption of methylene blue on zeolite was investigated by batch adsorption technique. The effect of different parameters such as zeolite dosage, initial methylene blue concentration, temperature, p^H and contact time on the adsorption process was discussed. Maximum adsorption capacity (4.31 mg/g) was achieved using 0.1 g of modified ZSM-5 zeolite at the optimum conditions (initial dye concentration: 10 mg/L, pH 10, temperature: 30 °C and contact time: 300 min). The experimental data were fitted into Langmuir and Freundlich models and the results indicate that the adsorption process followed Freundlich isotherm. Kinetic data were investigated using pseudo-first-order and pseudo-second-order models. Kinetic analysis indicates that pseudo-second-order model is more suitable to describe adsorption of MB on modified ZSM-5 zeolite. The reusability test suggests that the adsorbent could be reused at least six times without significant loss in removal efficiency.

Keywords ZSM-5 Zeolite · Poly (diallyl dimethylammonium chloride) · Methylene blue · Adsorption isotherm · Kinetics

Introduction

Water pollution has drastically increased in the last few decades due to the rapid growth of urbanisation and industrialization [1, 2]. Chemical industries such as textile, printing, paper, pharmaceutical, food, leather, photography, paints etc. are dumping tons and tons of untreated water to nearby lakes, rivers and sea and thereby accelerates the manmade water pollution [2–5]. Textile industries are one of the major contributors of water pollution and dispose large amount of toxic dyes to water bodies [6, 7]. Dyes are organic compounds which impart colour to the materials such as fabrics, paper, leather, food stuff etc. [8]. Based on their nuclear structures, dyes are classified into anionic, cationic and non-ionic dyes. Among them, cationic dye is known to be more toxic [8–10].

Methylene blue (MB) is a sapphire-coloured cationic dye which belongs to phenothiazine family (Fig. 1). It has been used as colorant, biological stain and redox indicator. However, due to its carcinogenic and mutagenic nature MB is considered as a harmful water pollutant [11, 12]. Hence researchers have implemented various physical, chemical and biological treatment methods for removing MB from water [13, 14]. Adsorption is one of the frequently used methods for removal of MB from aqueous solution. The interest in this technique mainly comes from its salient features such as low-cost, simplicity and easy handling [15–17]. There are several reports of using different adsorbent for the removal of MB from water [18–21]. For instance, Mouni et al. [22] reported that Algerian kaolin is an effective adsorbent for the removal of MB. The superior adsorption of kaolin is attributed to its high surface area. Huang et al. studied the removal efficiency of MB using graphene oxide

✉ Sabarish Radoor
sabarishchem@gmail.com

[1] Materials and Production Engineering, The Sirindhorn International Thai-German Graduate School of Engineering (TGGS), King Mongkut's University of Technology North Bangkok, Bangkok 10800, Thailand

[2] Government Women's Polytechnic College, Calicut, Kerala, India

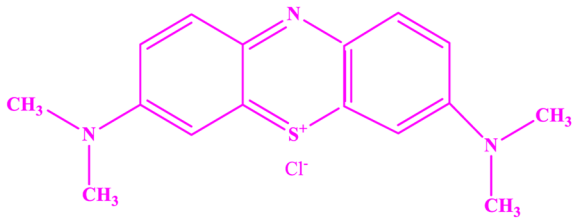

Fig. 1 Structural formula of methylene blue dye

modified zeolite [23] and kaolin [24]. The authors reported that the introduction of graphene oxide (GO) into zeolite/kaolin increases the active site on the composites and consequently improves its adsorption performance. Rida et al. [25] studies revealed that kaolin is a better adsorbent than zeolite for removing MB from aqueous solution. The high adsorption capacity (96%) of clay is attributed to its high surface area and pore diameter. Cao et al. [26] reported high MB removal efficiency and good regenerability of porous chitin. Aysan et al. [27] and co-workers employed chabazite to remove MB from aqueous environment and propose it as an excellent adsorbent for MB. Mayab et al. [28] successfully employed a low-cost bio adsorbent (walnut shell powder) to remove MB from aqueous solution.

Both natural and synthetic adsorbents have been successfully employed for the removal of dye from the aqueous effluents. Nevertheless, most of the adsorbents are expensive, toxic, non-biodegradable, poor in regeneration capability and selectivity. Therefore, finding a cost effective and biodegradable adsorbent is a relevant area of research [29–32]. Zeolites are naturally occurring crystalline aluminosilicate mineral with porous structure. Owing to its high surface area, pore volume and pore diameter, zeolites have been increasingly studied for the liquid adsorption of dissolved pollutants in water [33–36]. The characteristic properties of zeolites such as pore size, pore volume and surface area could be modified by different templates starch, cellulose, chitosan, agricultural waste etc. [37–40]. Previous studies indicate that uniform pores and well-defined surface area in modified zeolite is responsible for enhancing its adsorption efficiency [41–43] reported high dye removal efficiency of mesoporous ZSM-5 zeolite synthesized through templating method. Meanwhile, [44, 45] examined the dye removal ability of natural and modified zeolites. The adsorption studies suggest that modified zeolite is superior to unmodified zeolites.

In this context, it is worthwhile to develop a modified zeolite for the adsorption of MB dye. We have chosen poly (diallyl dimethyl ammonium chloride) (PDADMAC), bio polymer as template to generate mesoporosity in the zeolite system. The samples were characterized by Fourier-transform infrared spectroscopy, scanning electron microscopy, transmission electron microscopy, X-ray diffraction, N_2 adsorption analysis, thermogravimetric and ^{27}Al Nuclear Magnetic Resonance. The influence of different parameters such initial dye concentration, zeolite dosage, contact time, pH and temperature was investigated. The adsorption isotherm and kinetics of adsorption is also discussed.

Experimental Section

Materials

Poly (diallyl dimethyl ammonium chloride) solution [(PDADMAC); average M_w 200,000–350,000)], tetrapropyl ammonium hydroxide [$(CH_3CH_2CH_2)_4NOH$; TPAOH], tetraethyl orthosilicate ($C_8H_{20}O_4Si$; TEOS) and aluminium isopropoxide ($C_9H_{21}AlO_3$; AIP) were purchased from Sigma Aldrich Co. Ltd (India). Methylene blue ((MB, $C_{16}H_{18}ClN_3S$) used were procured from Merck, and were used without further purification.

Synthesis of Hierarchical Zeolite

The modified ZSM-5 zeolite was synthesized by employing hydrothermal crystallisation route. In a typical procedure, TEOS (3.46 g) and AIP (0.03 g) were mixed with stirring (300 rpm) to obtain a clear solution. To this, TPAOH (2.11 g) and PDADMAC (0.2 g) in aqueous solution was added and stirred for a whole day with controlled stirring (300 rpm), followed by rotavaporisation at 80 °C for 20 min. The transparent sticky solution thus obtained is transferred into autoclave and kept at 180 °C for 24 h. The synthesized zeolite was filtered, washed with water and later dried at 100 °C. Finally, the product was calcined in a muffle furnace at 550 °C for 5 h to remove the meso and micro templates from the framework. The PDADMAC modified ZSM-5 zeolite so obtained has been designated as PZSM-5. For comparison studies, we synthesized conventional ZSM-5 without adding meso template, and are denoted as ZSM-5 [40, 46–49]. Schematic representation of micro/mesopores formation in modified ZSM-5 zeolite is shown in Scheme 1.

Characterization

X-ray diffraction (XRD) patterns were obtained with a Rigaku Miniflex 2200 diffractometer using CuKα radiation. Scanning electron microscopic images were obtained by using a Hitachi SU6600 Variable Pressure Field Emission Scanning Electron Microscope (SEM). FT-IR spectrum was recorded in the range of 400–4000 cm^{-1} at room temperature using an FT-IR spectrometer (Jasco 4700). Thermogravimetric (TG) analysis of the uncalcined zeolite samples was done using a TGA (Instrument Q50) at a heating rate of 10 °C/

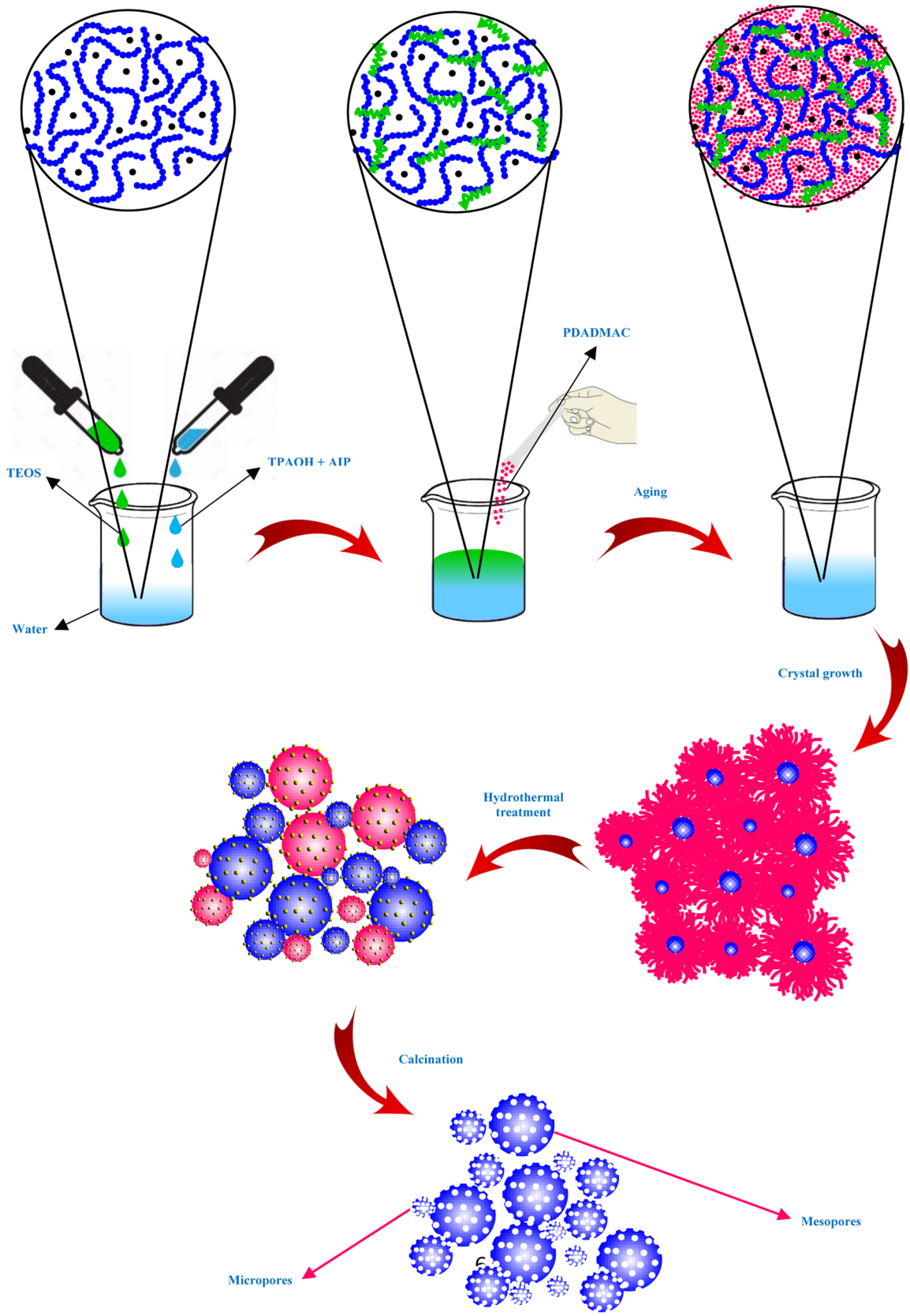

Scheme 1 Formation of micro/mesopores in modified ZSM-5 zeolite

min in nitrogen atmosphere. BET surface area and pore size distributions were measured using a Micromeritics Gemini V-2380 surface area analyser. Prior to the experiment, the samples were degassed at 200 °C under vacuum.^{27}Al MAS NMR spectra were recorded on a Bruker Avance AV 300 spectrometer. Transmission electron microscopic images (TEM) were obtained with a JEOL JEM-2100 transmission electron microscope operated at an accelerating voltage of 200 kV.

Adsorption Experiment

In the present work, we have compared the adsorption property of modified ZSM-5 zeolite with conventional zeolite. Adsorption studies were conducted by using 0.1 g of the modified/conventional ZSM-5 zeolite in 50 ml of MB solution. After regular time intervals, the MB solution was withdrawn and the absorbance of the solution was measured using UV–Vis spectrophotometer (Shimduzu 2500) at λ_{max} of 665 nm. The amount of MB adsorbed on the zeolite is calculated by the following equations.

$$q = \frac{(C_o - C_e)V}{W} \quad (1)$$

$$R(\%) = \frac{C_0 - C_e}{C_0} \times 100 \quad (2)$$

where, C_0 is the initial MB concentration in liquid (mg L^{-1}), Ce is the equilibrium MB concentration in liquid (mg L^{-1}), V is the volume of MB (L) and W is weight (g) of the zeolite.

The effect of adsorption parameters such as initial MB concentration, zeolite dosage, contact time, pH and temperature, were also investigated and is discussed below.

Regeneration of Adsorbents

An adsorbent with good regeneration capacity is always preferred for practical applications. Here we checked the regeneration ability of the modified zeolite for six recycle runs. For recycling, the dye adsorbed zeolite was soaked in HCl: ethanol mixture for few hours, washed several times with distilled water and dried at high temperature in hot air oven. The dried adsorbent was further used for next adsorption–desorption cycle [23].

Result and Discussion

Fourier-transform infrared spectra of conventional ZSM-5 and PDADMAC modified ZSM-5 zeolite are illustrated in Fig. 2 (I). A broad absorption peak appeared at 3800–3400 cm^{-1} is due to Si–OH and Al–OH groups in zeolite. In addition to this, we can also observe distinct peaks at 1225 cm^{-1} (external asymmetric stretch), 1100-1050 cm^{-1} (internal asymmetric stretching), 795 cm^{-1} (external symmetric stretching), 549 cm^{-1} (asymmetric stretching of double five-membered ring of MFI-type zeolites) and 450 cm^{-1} (internal tetrahedral bending) [50]. It is evident from Fig. 2 (1) that the spectra of conventional and PDADMAC modified ZSM-5 zeolite is identical and indicates the successful formation of MFI framework. The FTIR result also indicate that the added template (PDADMAC) does not distort the characteristic MFI structure of zeolite [51]. The XRD diffraction pattern of conventional and PDADMAC modified ZSM-5 are displayed in Fig. 2 (II). It can be clearly seen that both samples displayed characteristic peak at $2\theta = 7.98°$, 8.82°, 14.82°, 23.14°, 23.96° and 24.44° attributed to the reflection from.[011], [020], [031], [051], [303] and [313] plane of zeolites [52]. Absence of new diffraction peaks in PDADMAC modified ZSM-5 samples confirm the successful development of MFI structure in the sample. However, the crystallinity of PDADMAC modified zeolites is found to diminish slightly probably due to the disruption of the order structure of zeolite by PDADMAC or due to the presence of mesopores in the system (Noor et al. [53]). This result where in accordance with previous studies where the authors report a decline in intensity with the addition of templates [54]. Low crystallinity in the zeolite structure is advantageous for large molecular reactions as it improves the pore connectivity and facilitates the diffusion of large molecules.

The micro/meso structure of zeolite were analysed by SEM and TEM analysis. Figure 3 show the SEM images of conventional and PDADMAC modified ZSM-5. Conventional ZSM-5 displayed uniform surface with micropores while a rough surface with non-uniform distribution of micro/mesoporosity is clearly visible in the SEM micrograph of PDADMAC modified zeolite. TEM images is complimentary to SEM results and supports the formation of mesopores in PDADMAC modified zeolite. A well-defined lattice fringes seen in the SAED pattern of PDADMAC modified samples implies good crystallinity (Fig. 4) [55]. The thermogravimetric curves of conventional and PDADMAC modified ZSM-5 are shown in Fig. 5. Conventional ZSM-5 zeolite shows two thermal degradation at 100 and 360 °C, corresponding to the loss of water and structure directing agent (TPAOH) respectively. However, in the case of PDADMAC modified zeolite an additional weight loss at 290 °C is also observed. This is attributed to the loss of mesotemplate (PDADMAC) from the system. The high weight loss of PDADMAC modified ZSM-5 (42%) hint towards the presence of large pores in the modified sample [56]. Figure 6 illustrated the N_2 adsorption–desorption isotherm of conventional and PDADMAC modified ZSM-5 zeolite and their corresponding pore size distribution (inset

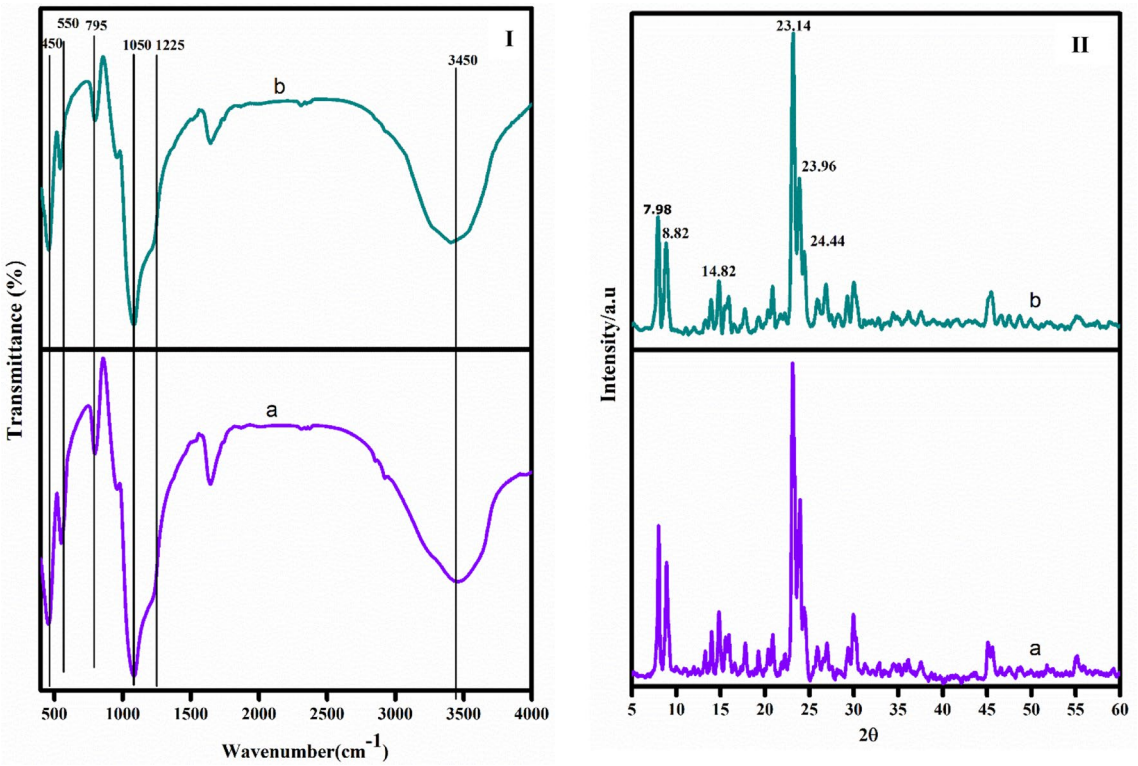

Fig. 2 I FTIR spectra and II XRD pattern of **a** CZSM-5 **b** PZSM-5

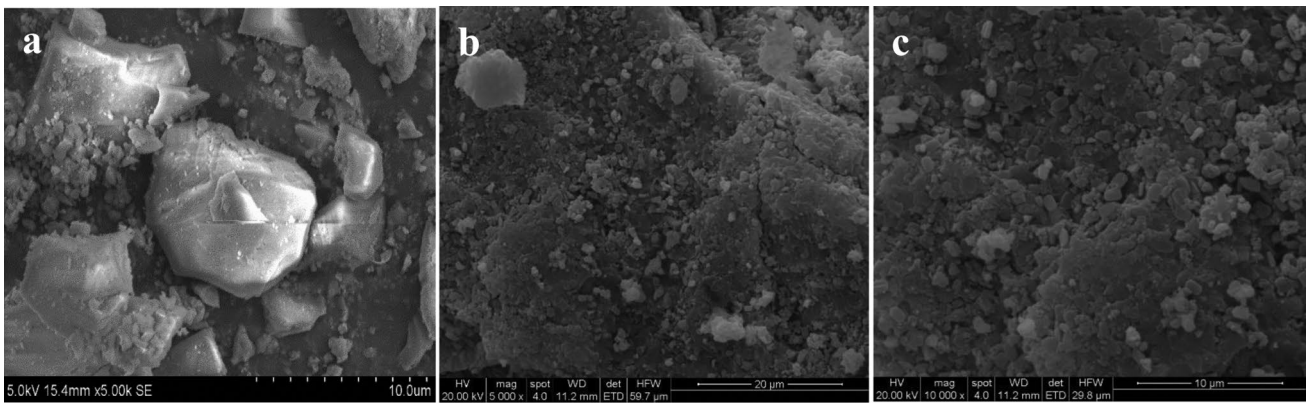

Fig. 3 SEM images of **a** CZSM-5 **b** and **c** PZSM-5

of Fig. 6 (II)). As can be seen from Fig. 6, the conventional ZSM-5 exhibits type-I isotherm (Langmuir isotherm) without any hysteresis loop implying the microporous structure. On contrary, we can observe type-IV isotherm with a broad hysteresis loop at a relative pressure (P/P_o) of 0.5–0.9 for PDADMAC modified ZSM-5 zeolite. This is attributed to capillary condensation of nitrogen and is characteristic of mesoporous systems. BJH pore size distribution of PDADMAC modified ZSM-5 revealed a prominent curve in the range of 10–30 nm, confirming the development of micro and mesopores in the system. The additional mesopores in the PDADMAC modified ZSM-5 is due to the removal of PDADMAC from the zeolite framework. The surface area and mesopore volume of conventional and hierarchical zeolite is displayed in Table 1. It can be seen that the PDADMAC templated sample possess high surface area and mesopore volume than conventional zeolite (440 m^2/g and 0.44 cm^3/g), respectively, which were much larger than those of other ZSM-5 catalysts (Table 1). Therefore, PDADMAC modified zeolite has high pore volume than conventional

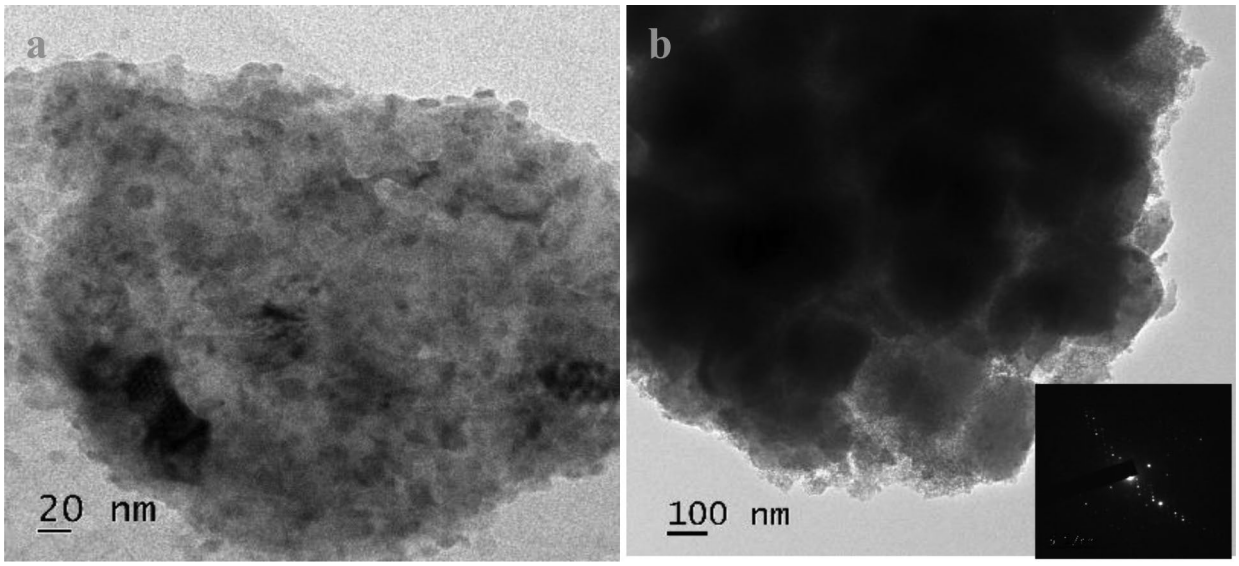

Fig. 4 TEM images of PZSM-5

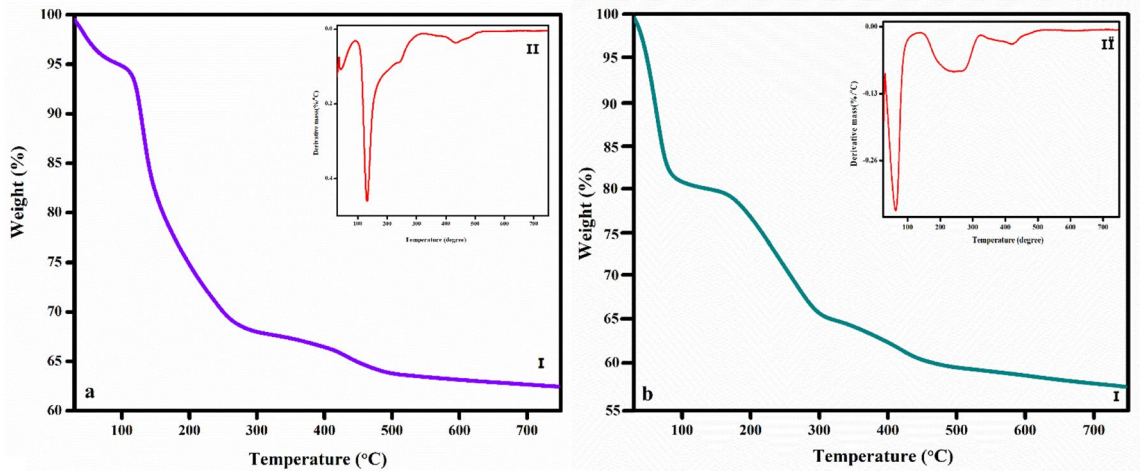

Fig. 5 Thermogravimetric curve of: **a** CZSM-5 **b** PZSM-5 (DTG curves are given at the inset)

ZSM-5 thus suggesting a superior adsorption power for the system.^{27}Al NMR spectra for PDADMAC modified ZSM-5 zeolites are shown in Fig. 7. We can observe two distinct signals: one at chemical shifts of ~ 54 ppm and the second at ~ 0 ppm. The peak observed at ~ 54 ppm and ~ 0 ppm corresponds to the tetrahedral and octahedral aluminium in the framework of zeolite. The ^{27}Al NMR analysis thus confirms that most of the Al species are tetrahedrally and octahedrally coordinated in the framework [57].

Adsorption Studies

An idea of optimum adsorbent dosage is essential for large scale industrial applications. So, we have varied the zeolite dosage from 0.025 to 0.1 g by keeping other parameters constant. The effect of zeolite dosage on the adsorption of MB is graphically depicted in Fig. 8a. From the figure, one can see that on increasing the zeolite amount from 0.025 to 0.1 g, the adsorption capacity increases from 2.9 to 4.31 mg/g. This could be due to enhancement in the total surface area of the system which promotes the adherence of MB on the surface of zeolite. Since PDADMAC modified zeolite contain mesopores, an enhancement in its dosage could have increase the number of mesopores in the system and thus facilitates the penetration of large MB molecules [58]. The effect of contact time for the uptake of MB by modified zeolite was examined and the result is illustrated in Fig. 8b. It is evident that the adsorption take

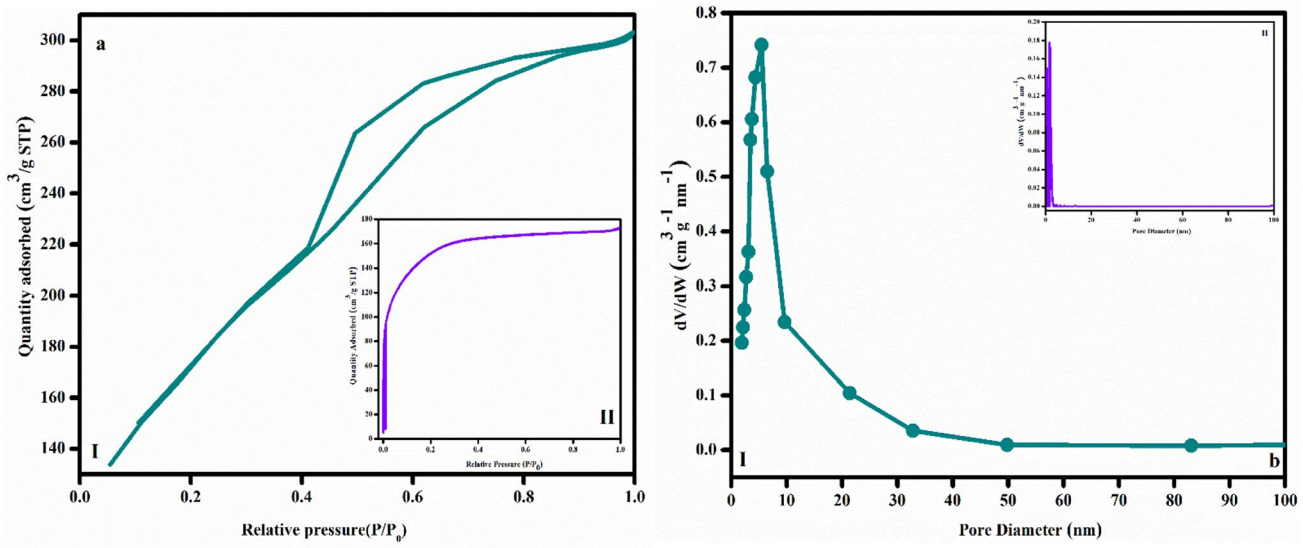

Fig. 6 **a** Nitrogen adsorption–desorption isotherms of (i) PZSM-5 (ii) (inset) CZSM-5; **b** Pore size distribution curve of: (i) PZSM-5 (ii) (inset) CZSM-5

Table 1 Textural characteristics of conventional and PDADMAC modified ZSM-5 zeolite

Sample	S_{BET} ($m^2\ g^{-1}$)	V_{total} ($cm^3\ g^{-1}$)	V_{meso} ($cm^3\ g^{-1}$)
PZSM-5	440	0.44	0.31
CZSM-5	344	0.37	0.083

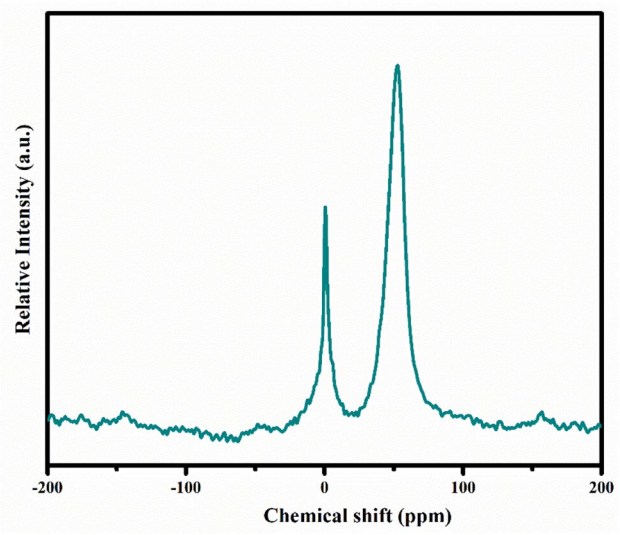

Fig. 7 Solid state ^{27}Al NMR spectra of PZSM-5

place in two stage. In the first stage, the adsorption capacity increases rapidly with contact time, probably due to the availability of large number of active sites. Meanwhile, in the second stage, only a slow increase in the adsorption capacity with contact time was observed and after 4 h the adsorption attains equilibrium. This may be allocated to the fact that the number of available adsorption site on the surface of zeolite decreases with contact time and eventually all adsorption sites will be occupied by MB molecule. Therefore, all experiments were conducted at a contact time of 4 h. In order to evaluate the effect of initial concentration of MB on modified ZSM-5 we have varied the initial concentration from 10 to 50 ppm. It is revealed that adsorption capacity increases with initial dye concentration but the removal percentage decreases. On increasing MB concentration, the mass driving force for the transfer of MB from solid to liquid phase increases and thus leads to enhancement in the adsorption capacity. The reduction in the removal percentage could be due to the decline in the ratio of number of available adsorption site to the number of MB molecules (Fig. 8c). This trend is in agreement with previous reports [59]. pH is an important factor that influence the adsorption process, so in this present work, adsorption of MB dye on zeolite have been studied at different pH (2–10) and is displayed in Fig. 8d. At low pH, due to the possible protonation, the surface of adsorbent becomes positive charged and thus repel the incoming MB molecule. However, at high pH, the surface becomes negative and thus provide a favourable condition (electrostatic attraction) for the attachment of MB molecule on surface of zeolite. From the above studies, it can be concluded that low pH disfavours the adsorption of MB on zeolite while high pH favours the adsorption process. Finally, we monitored the adsorption capacity as a function of temperature and is displayed shown in Fig. 8e. It is clear from Fig. 8e that upon increasing the temperature

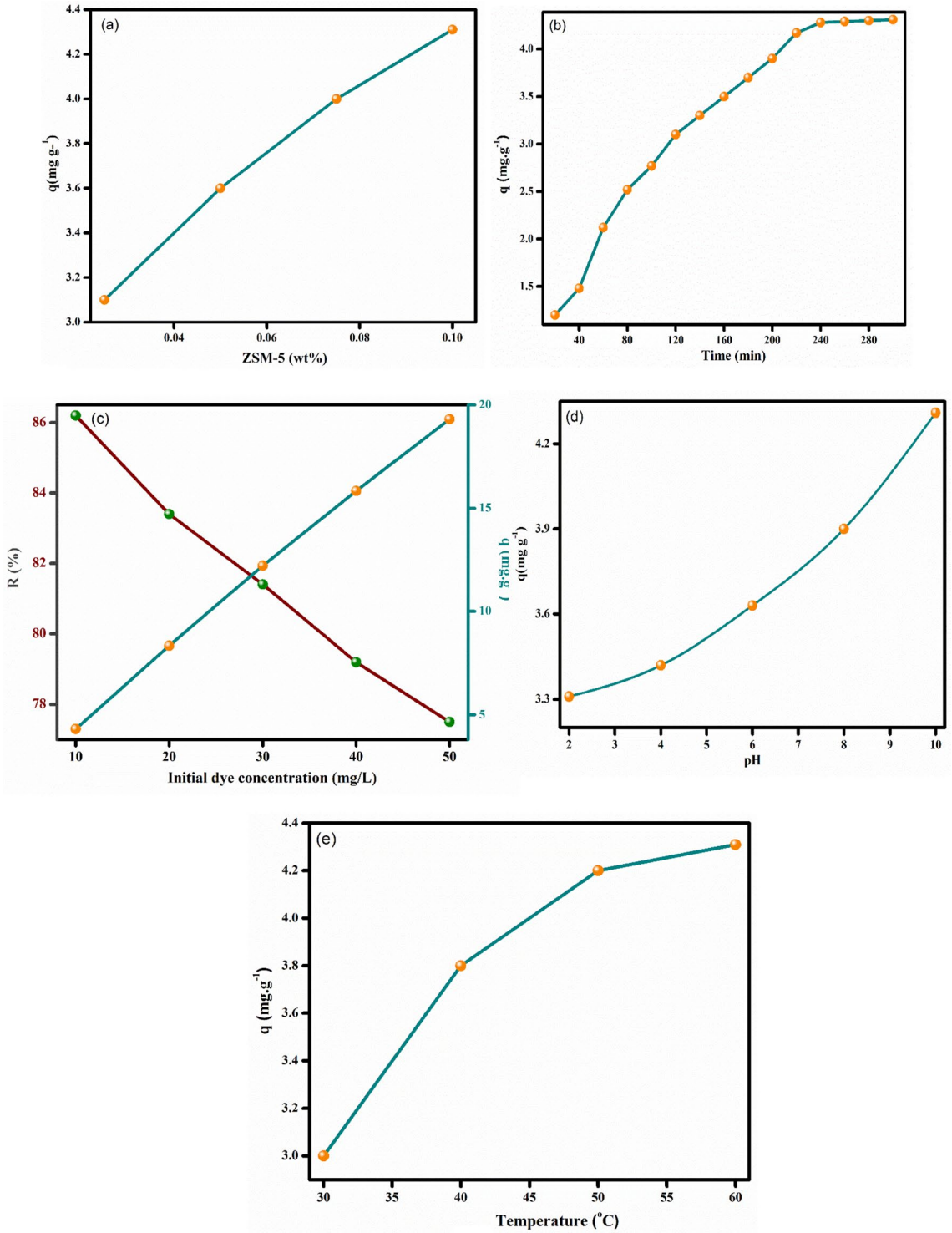

Fig. 8 Effect of different parameters **a** zeolite dosage; **b** contact time; **c** initial dye concentration; **d** pH; **e** temperature on adsorption of MB on PDADMAC modified ZSM-5

the adsorption capacity slightly increases, implying an endothermic nature of the adsorption process. Another plausible reason is that thermal energy provides a favourable driving force for the diffusion of large MB molecule from liquid solution into the solid adsorbent.

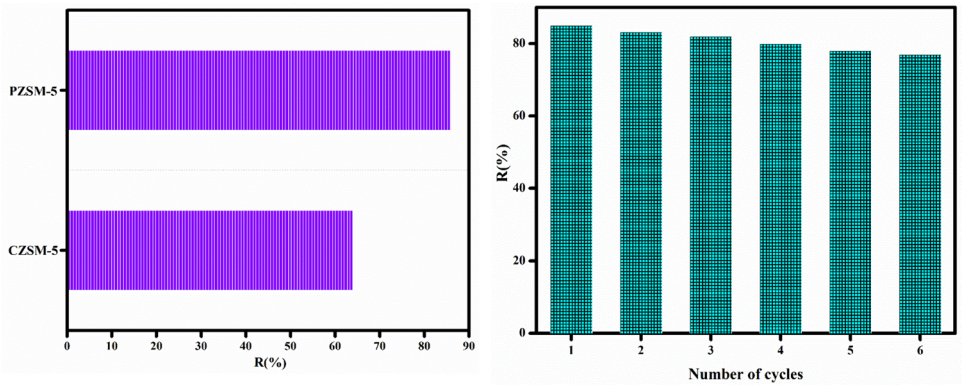

Fig. 9 Effect of different type of zeolite and reusability of MB dye on PDADMAC modified ZSM-5

Comparison between PDADMAC Modified and Conventional ZSM-5

Figure 9 illustrates the comparison of adsorption performance of PDADMAC modified ZSM-5 zeolite with conventional ZSM-5 zeolite. It can be seen that PDADMAC modified zeolite exhibits high adsorption capacity than conventional zeolite, probably due to the difference in the porosity, which is evident from morphological and BET analysis. In the case of conventional zeolite, only surface adsorption is possible, as the small micropores in it will restrict the penetration of large MB molecules. However, mesopores in PDADMAC modified zeolite facilitates the penetration of large MB molecules and thus offer a higher

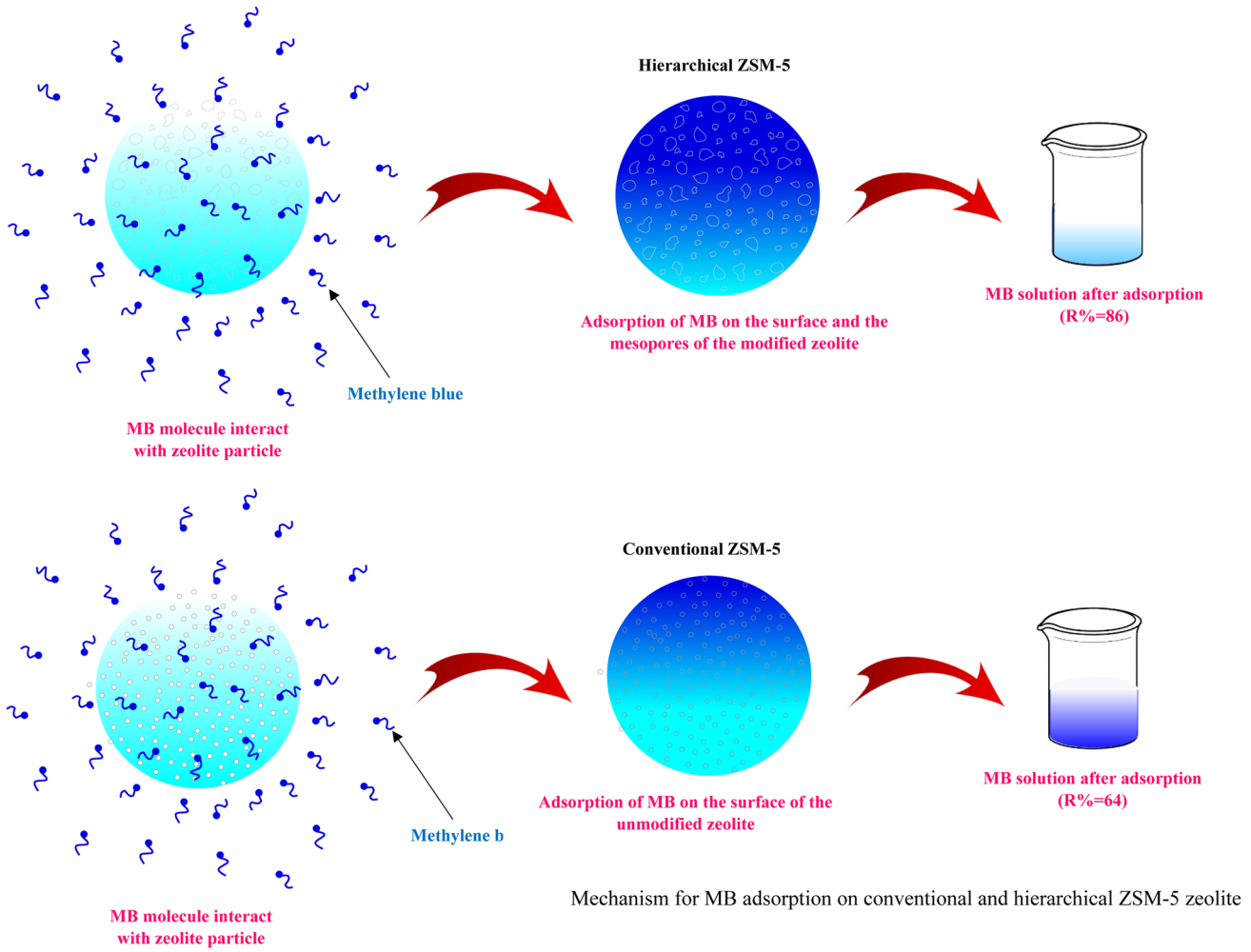

Scheme 2 Mechanism for MB adsorption on conventional and hierarchical ZSM-5 zeolite

adsorption capacity than conventional zeolite. This is schematically represented in Scheme 2.

Reusability

An adsorbent with good regeneration ability is always recommended for the treatment of water treatment. In the present work, the regeneration capacity of PDADMAC modified zeolite was checked for six adsorption–desorption cycle. From Fig. 9 it is clear that the adsorption capacity of zeolite slightly reduced with number of cycles. Nevertheless, even after 6 recycle it possess good removal efficiency thus suggesting it as a potential candidate for dye removal application.

Adsorption Kinetics

Kinetic models were employed to understand the rate and mechanism of adsorption. In the present study, the kinetics of MB adsorption onto PDADMAC modified zeolite was evaluated by applying pseudo-first-order (PFO) and pseudo-second-order (PSO) model. The differential form of pseudo-first-order model is represented as

$$\frac{dq_t}{dt} = K_1(q_e - q_t) \tag{3}$$

where q_t (mg/g) is the amount of MB adsorbate on the surface of PDADMAC modified zeolite at time t, q_e is the equilibrium adsorption capacity (mg/g). K_1 is pseudo-first-order rate constant (L min^{-1}). The linearized form of Eq. 3 is represented as

$$\log(q_e - q_t) = \log q_e - \frac{K_1 t}{2.303} \tag{4}$$

The kinetic parameter K_1 and q_e were obtained from the linear fit of log $(q_e - q_t)$ against time.

The PSO model is represented as

$$\frac{dq_t}{dt} = K_1(q_e - q_t)^2 \tag{5}$$

The Eq. (5) is integrated by applying boundary condition and on rearranging gives the linearized form which is represented as follows

$$\frac{t}{q_e} = \frac{1}{K_2 q_e^2} + \frac{t}{q_e} \tag{6}$$

where K_2 is the rate constant of PSO (g/mg min). The value of q_e and K_2 can be calculated from the linear plot of t/qt vs time.

The goodness of fit (correlation coefficient R^2) is used to identify the best kinetic model for adsorption process. Kinetic model with high correlation coefficient (R^2) value is usually selected as the best model for a particular adsorption reaction [60, 61]. In order to identify the kinetic model, we have fitted the experimental data into PFO and PSO. The linear fitted graph is shown in Fig. 10 and the kinetic parameters are summarized in Table 2. On comparing the linear plot and R^2, one can observe that PSO model has best agreement with the experimental adsorption data and is most suitable to describe MB adsorption on zeolite.

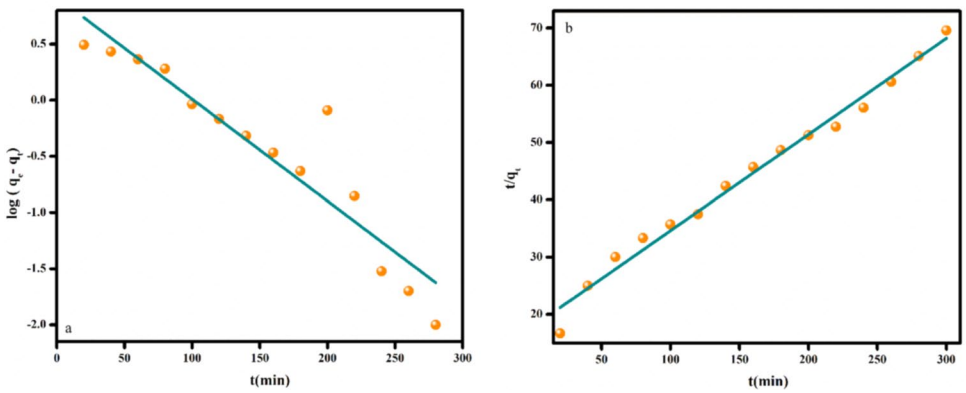

Fig. 10 Linear kinetic plots of **a** pseudo-first-order **b** pseudo-second-order models for the adsorption of MB dye for the PDADMAC modified ZSM-5 zeolite

Table 2 Adsorption kinetic parameters and correlation coefficient for the adsorption of MB dye on modified ZSM-5 zeolite with PFO and PSO

Exp	Pseudo-first-order			Pseudo-second-order		
q_e, exp (mg g^{-1})	K_1	q_e(mg g^{-1})	R^2	K_2 (g mg^{-1} min^{-1})	q_e(mg g^{-1})	R^2
4.31	−0.0218	10	0.93	0.00157	4.8	0.999

Table 3 Comparison study of MB on different adsorbent

Adsorbents	q_{max} (mg/g)	References
Graphite oxide	0.74	[66]
Cotton alk	0.024	[67]
Coal fly ash	2.88	[35]
Acid-activated milled pyrophylite	4.2	[68]
Perlite	0.7	[69]
AC-apricot shell	4.11	[70]
PDADMAC modified zeolite	4.31	This work

Adsorption Isotherm

Adsorption isotherm describes the interaction between adsorbent and adsorbate and elucidates the adsorption mechanism. The experiment data of MB on PDADMAC modified ZSM-5 zeolite was analysed using two well-known models; Langmuir and Freundlich isotherms.

The Langmuir isotherm assumes an equivalent adsorption site on the surface of adsorbent and neglects any interaction between the adsorbed molecules. Thus, it suggests monolayer formation on the surface of the adsorbent. The linear form of Langmuir equation can be described as

$$\frac{C_e}{q_e} = \left(\frac{C_e}{q_{max}}\right) + \left(\frac{1}{K_L * q_{max}}\right) \quad (7)$$

where K_L is Langmuir constant, C_e is equilibrium dye concentration (mg/L), q_e is the amount of dye adsorbed onto the ZSM-5 (mg/g) and q_{max} is maximum adsorption (mg/g). The linear plot of C_e/q_e against C_e gives a straight with slope $1/q_m$ and intercept $1/q_m K_L$. R_L (equilibrium parameter) is another characteristic parameter obtained from Langmuir isotherm model and is used to predict the favorability of the adsorption process. The value of R_L between 0 and 1 is considered as favorable for the adsorption process.

The Freundlich model assumes multilayer adsorption on a heterogenous surface. The linear form of Freundlich equation can be expressed as follows;

$$\ln(q_e) = \ln K_F + \frac{1}{n} * \ln(C_e) \quad (8)$$

where K_F is Freundlich constant (mg/g) $(L/mg)^{1/n}$) and n is the heterogeneity factor. K_F is related to the adsorption capacity and 'n' indicates the feasibility of adsorption. Adsorption process is considered to be favorable if the value of 1/n is between 0 and 1 [62–65].

Comparison with Other Adsorbent

From the Table 3, it is clear that the hierarchical ZSM-5 possess fairly good adsorption capacity and its comparable with other adsorbents. Hence, PDADMAC modified ZSM-5 zeolite could be a promising candidate for the removal of MB from aqueous solutions

The plot of ln q_e versus ln C_e and C_e/qe versus C_e for MB adsorption on PDADMAC modified ZSM-5 zeolite is shown in Fig. 11 and the corresponding adsorption

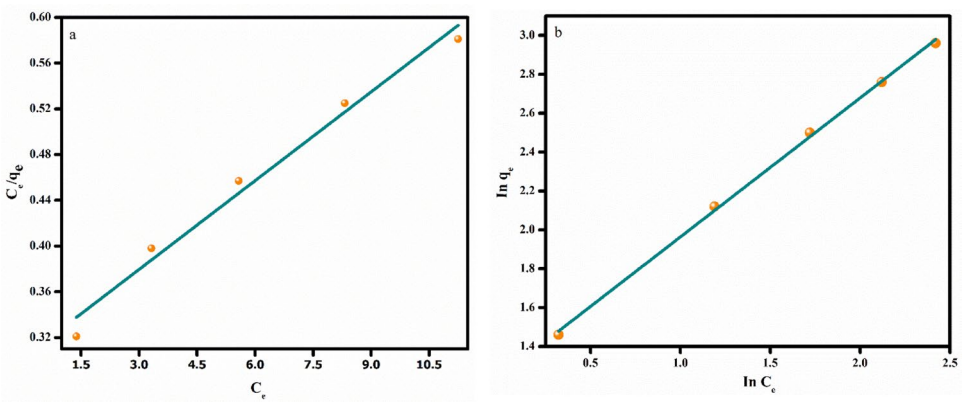

Fig. 11 Linear isotherm plots of **a** Langmuir **b** Freundlich model for the adsorption of MB dye for the PDADMAC modified ZSM-5 zeolite

Table 4 Adsorption isotherm parameters and correlation coefficient for the adsorption of MB dye on modified ZSM-5 zeolite with Langmuir and Freundlich

Exp	Langmuir isotherm			Freundlich isotherm		
q_e, exp (mg g^{-1})	R^2	q_{max}(mg g^{-1})	K_L	R^2	K_F (mg g^{-1})	n
4.31	0.98	38	0.085	0.999	3.8	1.4

parameter are displayed in Table 4. As can be seen Fig. 11 the experimental data fitted well in the Freundlich model with a high regression coefficient value (0.99). The value of 1/n is found to be (0.714) implying a favorable adsorption. Thus, MB molecules is distributed in multilayer fashion on the surface of PDADMAC modified zeolite.

Conclusion

A modified ZSM-5 zeolite was successfully developed by using PDADMAC as the mesotemplate. The crystallinity and chemical structure of synthesised zeolite is confirmed by XRD and FTIR analysis. N_2 adsorption and morphological analysis confirms the generation of mesopores in the PDADMAC modified samples. Adsorption studies indicate that PDADMAC modified ZSM-5 zeolite is as good adsorbent for the removal of cationic dye MB, from aqueous solution. The result further shows that adsorption process could be tuned by varying the operation parameters such as zeolite dosage, initial dye concentration, contact time, temperature and pH. Optimized conditions for removal efficiency are as follows (modified ZSM-5 zeolite:0.1 g, initial dye concentration:10 mg/L, pH: 10 and contact time: 300 min). The adsorption isotherm and kinetic studies indicate that Freundlich model and pseudo-second-order model is the best model to explain MB adsorption onto PDADMAC modified zeolite. The recyclability results suggest that PDADMAC modified ZSM-5 zeolite possess good regeneration capacity. Thus, we propose PDADMAC modified ZSM-5 zeolite as a potential adsorbent for removing methylene blue from water.

Acknowledgements The authors are grateful to the King Mongkut's University of Technology North Bangkok (KMUTNB), Thailand and grant funded the Post-Doctoral scholarship ((Grant No. KMUTNB-63-Post-03 to SR) and (Grant No. KMUTNB-64-03, KMUTNB-BasicR-64-16). For further information on what should be included under each heading, please select the Instructions for Author link.

Author Contribution SR- Conceptualization, Methodology, Investigation, Validation, Writing—original draft, Software, Writing—review and editing, Formal analysis; JK – Investigation, Analysis, Interpretation of results, Software, Writing – review and editing, Formal analysis; AJ—Data collection, Validation, Writing—review and editing, Formal analysis; JP –Validation, Software, Writing—review and editing and Investigation; SS – Editing, Funding and Supervision.

Funding (Grant No. KMUTNB-63-Post-03 to SR) and (Grant No. KMUTNB-64-03, KMUTNB-BasicR-64-16).

Data Availability All data generated or analysed during this study are included in this published article.

Compliance with Ethical Standards

Conflict of interest The authors don't have any conflicts of interests.

Ethical Approval The article we have submitted to the journal for review is original, has been written by the stated authors and has not been published elsewhere. The images that we have submitted to the journal for review are original, and has not been published elsewhere.

Consent to Participate This manuscript has not been submitted to, nor is under review at, another journal or other publishing venue. The authors have no affiliation with any organization with a direct or indirect financial interest in the subject matter discussed in the manuscript.

Consent for Publication The authors confirm the consent for publication.

References

1. Dil EA, Ghaedi M, Ghezelbash GR, Asfaram A, Ghaedi AM, Mehrabi F (2016) Modeling and optimization of Hg2+ ion biosorption by live yeast Yarrowia lipolytica 70562 from aqueous solutions under artificial neural network-genetic algorithm and response surface methodology: kinetic and equilibrium study. RSC Adv 6(59):54149–54161. https://doi.org/10.1039/c6ra11292g
2. Sharifpour E, Khafri HZ, Ghaedi M, Asfaram A, Jannesar R (2018) Isotherms and kinetic study of ultrasound-assisted adsorption of malachite green and Pb2+ ions from aqueous samples by copper sulfide nanorods loaded on activated carbon: experimental design optimization. Ultrason Sonochem 40:373–382. https://doi.org/10.1016/j.ultsonch.2017.07.030
3. Kumari S, Khan AA, Chowdhury A, Bhakta AK, Mekhalif Z, Hussain S (2020) Efficient and highly selective adsorption of cationic dyes and removal of ciprofloxacin antibiotic by surface modified nickel sulfide nanomaterials: kinetics, isotherm and adsorption mechanism. Colloids Surf A. https://doi.org/10.1016/j.colsurfa.2019.124264
4. Sun H, Cao L, Lu L (2011) Magnetite/reduced graphene oxide nanocomposites: one step solvothermal synthesis and use as a novel platform for removal of dye pollutants. Nano Res 4(6):550–562. https://doi.org/10.1007/s12274-011-0111-3
5. Wang XS, Zhou Y, Jiang Y, Sun C (2008) The removal of basic dyes from aqueous solutions using agricultural by-products. J Hazard Mater 157(2–3):374–385. https://doi.org/10.1016/j.jhazmat.2008.01.004
6. Talaiekhozani A, Reza Mosayebi M, Fulazzaky MA, Eskandari Z, Sanayee R (2020) Combination of TiO2 microreactor and electroflotation for organic pollutant removal from textile dyeing industry wastewater. Alexandria Eng J 59(2):549–563. https://doi.org/10.1016/j.aej.2020.01.052
7. Tkaczyk A, Mitrowska K, Posyniak A (2020) Synthetic organic dyes as contaminants of the aquatic environment and their implications for ecosystems: a review. Sci Total Environ. https://doi.org/10.1016/j.scitotenv.2020.137222
8. Adegoke KA, Bello OS (2015) Dye sequestration using agricultural wastes as adsorbents. Water Resour Ind 12:8–24. https://doi.org/10.1016/j.wri.2015.09.002
9. Alver E, Metin AÜ (2012) Anionic dye removal from aqueous solutions using modified zeolite: adsorption kinetics and isotherm studies. Chem Eng J 200–202:59–67. https://doi.org/10.1016/j.cej.2012.06.038
10. Mall ID, Srivastava VC, Agarwal NK (2006) Removal of orange-G and methyl Violet dyes by adsorption onto bagasse fly ash—kinetic study and equilibrium isotherm analyses. Dyes Pigm 69(3):210–223. https://doi.org/10.1016/j.dyepig.2005.03.013

11. Khodaie M, Ghasemi N, Moradi B, Rahimi M (2013) Removal of methylene blue from wastewater by adsorption onto ZnCl2 activated corn husk carbon equilibrium studies. J Chem 2013:1–6. https://doi.org/10.1155/2013/383985
12. Naushad M, Alqadami AA, AlOthman ZA, Alsohaimi IH, Algamdi MS, Aldawsari AM (2019) Adsorption kinetics, isotherm and reusability studies for the removal of cationic dye from aqueous medium using arginine modified activated carbon. J Mol Liq. https://doi.org/10.1016/j.molliq.2019.111442
13. Sizmur T, Fresno T, Akgül G, Frost H, Moreno-Jiménez E (2017) Biochar modification to enhance sorption of inorganics from water. Biores Technol 246:34–47. https://doi.org/10.1016/j.biortech.2017.07.082
14. Zhao B, O'Connor D, Zhang J, Peng T, Shen Z, Tsang DCW, Hou D (2018) Effect of pyrolysis temperature, heating rate, and residence time on rapeseed stem derived biochar. J Clean Prod 174:977–987. https://doi.org/10.1016/j.jclepro.2017.11.013
15. Benkhaya S, Achiou B, Ouammou M, Bennazha J, Alami Younssi S, M'rabet S, El Harfi A (2019) Preparation of low-cost composite membrane made of polysulfone/polyetherimide ultrafiltration layer and ceramic pozzolan support for dyes removal. Mater Today Commun 19:212–219. https://doi.org/10.1016/j.mtcomm.2019.02.002
16. Nas MS, Calimli MH, Burhan H, Yılmaz M, Mustafov SD, Sen F (2019) Synthesis, characterization, kinetics and adsorption properties of Pt-Co@GO nano-adsorbent for methylene blue removal in the aquatic mediums using ultrasonic process systems. J Mol Liq. https://doi.org/10.1016/j.molliq.2019.112100
17. Vakili M, Deng S, Cagnetta G, Wang W, Meng P, Liu D, Yu G (2019) Regeneration of chitosan-based adsorbents used in heavy metal adsorption: a review. Sep Purif Technol 224:373–387. https://doi.org/10.1016/j.seppur.2019.05.040
18. Jawad AH, Abdulhameed AS (2020) Mesoporous Iraqi red kaolin clay as an efficient adsorbent for methylene blue dye: adsorption kinetic, isotherm and mechanism study. Surf Interfaces. https://doi.org/10.1016/j.surfin.2019.100422
19. Pang X, Sellaoui L, Franco D, Netto MS, Georgin J, Luiz Dotto G, Li Z (2020) Preparation and characterization of a novel mountain soursop seeds powder adsorbent and its application for the removal of crystal violet and methylene blue from aqueous solutions. Chem Eng J. https://doi.org/10.1016/j.cej.2019.123617
20. Pomicpic J, Dancel GC, Cabalar PJ, Madrid J (2020) Methylene blue removal by poly(acrylic acid)-grafted pineapple leaf fiber/polyester nonwoven fabric adsorbent and its comparison with removal by gamma or electron beam irradiation. Radiat Phys Chem. https://doi.org/10.1016/j.radphyschem.2020.108737
21. Shooto ND, Thabede PM, Bhila B, Moloto H, Naidoo EB (2020) Lead ions and methylene blue dye removal from aqueous solution by mucuna beans (velvet beans) adsorbents. J Environ Chem Eng. https://doi.org/10.1016/j.jece.2019.103557
22. Mouni L, Belkhiri L, Bollinger J-C, Bouzaza A, Assadi A, Tirri A, Remini H (2018) Removal of methylene blue from aqueous solutions by adsorption on kaolin: kinetic and equilibrium studies. Appl Clay Sci 153:38–45. https://doi.org/10.1016/j.clay.2017.11.034
23. Huang T, Yan M, He K, Huang Z, Zeng G, Chen A, Chen G (2019) Efficient removal of methylene blue from aqueous solutions using magnetic graphene oxide modified zeolite. J Colloid Interface Sci 543:43–51. https://doi.org/10.1016/j.jcis.2019.02.030
24. He K, Chen G, Zeng G, Chen A, Huang Z, Shi J, Hu L (2018) Enhanced removal performance for methylene blue by kaolin with graphene oxide modification. J Taiwan Inst Chem Eng 89:77–85. https://doi.org/10.1016/j.jtice.2018.04.013
25. Rida K, Bouraoui S, Hadnine S (2013) Adsorption of methylene blue from aqueous solution by kaolin and zeolite. Appl Clay Sci 83–84:99–105. https://doi.org/10.1016/j.clay.2013.08.015
26. Cao Y-L, Pan Z-H, Shi Q-X, Yu J-Y (2018) Modification of chitin with high adsorption capacity for methylene blue removal. Int J Biol Macromol 114:392–399. https://doi.org/10.1016/j.ijbiomac.2018.03.138
27. Aysan H, Edebali S, Ozdemir C, Celïk Karakaya M, Karakaya N (2016) Use of chabazite, a naturally abundant zeolite, for the investigation of the adsorption kinetics and mechanism of methylene blue dye. Microporous Mesoporous Mater 235:78–86. https://doi.org/10.1016/j.micromeso.2016.08.007
28. Miyah Y, Lahrichi A, Idrissi M, Khalil A, Zerrouq F (2018) Adsorption of methylene blue dye from aqueous solutions onto walnut shells powder: equilibrium and kinetic studies. Surf Interfaces 11:74–81. https://doi.org/10.1016/j.surfin.2018.03.006
29. Aichour A, Zaghouane-Boudiaf H (2019) Highly brilliant green removal from wastewater by mesoporous adsorbents: kinetics, thermodynamics and equilibrium isotherm studies. Microchem J 146:1255–1262. https://doi.org/10.1016/j.microc.2019.02.040
30. Shittu I, Achazhiyath Edathil A, Alsaeedi A, Al-Asheh S, Polychronopoulou K, Banat F (2019) Development of novel surfactant functionalized porous graphitic carbon as an efficient adsorbent for the removal of methylene blue dye from aqueous solutions. J Water Process Eng 28:69–81. https://doi.org/10.1016/j.jwpe.2019.01.001
31. Soliman N, MoustafaAboudHalim AFAAKSA (2019) Effective utilization of Moringa seeds waste as a new green environmental adsorbent for removal of industrial toxic dyes. J Mater Res Technol 8(2):1798–1808. https://doi.org/10.1016/j.jmrt.2018.12.010
32. Ullah R, Sun J, Gul A, Bai S (2020) One-step hydrothermal synthesis of TiO2-supported clinoptilolite: an integrated photocatalytic adsorbent for removal of crystal violet dye from aqueous media. J Environ Chem Eng. https://doi.org/10.1016/j.jece.2020.103852
33. Guo Y-P, Wang H-J, Guo Y-J, Guo L-H, Chu L-F, Guo C-X (2011) Fabrication and characterization of hierarchical ZSM-5 zeolites by using organosilanes as additives. Chem Eng J 166(1):391–400. https://doi.org/10.1016/j.cej.2010.10.057
34. Han R, Zhang J, Han P, Wang Y, Zhao Z, Tang M (2009) Study of equilibrium, kinetic and thermodynamic parameters about methylene blue adsorption onto natural zeolite. Chem Eng J 145(3):496–504. https://doi.org/10.1016/j.cej.2008.05.003
35. Jin X, Jiang M-q, Shan X-q, Pei Z-g, Chen Z (2008) Adsorption of methylene blue and orange II onto unmodified and surfactant-modified zeolite. J Colloid Interface Sci 328(2):243–247. https://doi.org/10.1016/j.jcis.2008.08.066
36. Wang S, Zhu Z (2006) Characterisation and environmental application of an Australian natural zeolite for basic dye removal from aqueous solution. J Hazard Mater 136(3):946–952. https://doi.org/10.1016/j.jhazmat.2006.01.038
37. Jin J, Zhang X, Li Y, Li H, Wu W, Cui Y, Shi J (2012) A simple Route to synthesize mesoporous ZSM-5 templated by ammonium-modified chitosan. Chem Eur J 18(51):16549–16555. https://doi.org/10.1002/chem.201201614
38. Krishnamurthy M, Msm K, Kanakkampalayam KC (2016) Hierarchically structured MFI zeolite monolith prepared using agricultural waste as solid template. Microporous Mesoporous Mater 221:23–31. https://doi.org/10.1016/j.micromeso.2015.09.022
39. Sabarish R, Unnikrishnan G (2017) Synthesis, characterization and catalytic activity of hierarchical ZSM-5 templated by carboxymethyl cellulose. Powder Technol 320:412–419. https://doi.org/10.1016/j.powtec.2017.07.041
40. Sabarish R, Unnikrishnan G (2019) Synthesis, characterization and evaluations of micro/mesoporous ZSM-5 zeolite using starch as bio template. SN Appl Sci. https://doi.org/10.1007/s42452-019-1036-9

41. Drumm FC, Oliveira JSD, Enders MSP, Müller EI, Urquieta-González EA, Dotto GL, Jahn SL (2018) Use of chitin as a template for the preparation of mesostructured ZSM-5. Cerâmica 64(370):214–218. https://doi.org/10.1590/0366-69132018643702271
42. Radoor S, Karayil J, Parameswaranpillai J, Siengchin S (2020) Adsorption study of anionic dye, eriochrome black t from aqueous medium using polyvinyl alcohol/starch/ZSM-5 zeolite membrane. J Polym Environ 28(10):2631–2643. https://doi.org/10.1007/s10924-020-01812-w
43. Sari ZGLV, Younesi H, Kazemian H (2014) Synthesis of nanosized ZSM-5 zeolite using extracted silica from rice husk without adding any alumina source. Appl Nanosci 5(6):737–745. https://doi.org/10.1007/s13204-014-0370-x
44. Armagan B, Turan M, Karadag D (2010) Adsorption of different reactive dyes onto surfactant-modified zeolite: kinetic and equilibrium modeling. In Survival and Sustainability, pp. 1237–1254
45. Armağan B, Turan M, Özdemir O, Çelik MS (2004) Color removal of reactive dyes from water by Clinoptilolite. J Environ Sci Health Part A 39(5):1251–1261. https://doi.org/10.1081/ese-120030329
46. Radoor S, Karayil J, Jayakumar A, Parameswaranpillai J, Siengchin S (2021) An efficient removal of malachite green dye from aqueous environment using ZSM-5 zeolite/polyvinyl alcohol/carboxymethyl cellulose/sodium alginate bio composite. J Polym Environ. https://doi.org/10.1007/s10924-020-02024-y
47. Radoor S, Karayil J, Parameswaranpillai J, Siengchin S (2020) Removal of anionic dye Congo red from aqueous environment using polyvinyl alcohol/sodium alginate/ZSM-5 zeolite membrane. Sci Rep. https://doi.org/10.1038/s41598-020-72398-5
48. Sabarish R, Jasila K, Aswathy J, Jyotishkumar P, Suchart S (2020) Fabrication of PVA/agar/modified ZSM-5 zeolite membrane for removal of anionic dye from aqueous solution. Int J Environ Sci Technol. https://doi.org/10.1007/s13762-020-02998-1
49. Sabarish R, Unnikrishnan G (2020) A novel anionic surfactant as template for the development of hierarchical ZSM-5 zeolite and its catalytic performance. J Porous Mater 27(3):691–700. https://doi.org/10.1007/s10934-019-00852-5
50. Narayanan S, Vijaya JJ, Sivasanker S, Ragupathi C, Sankaranarayanan TM, Kennedy LJ (2016) Hierarchical ZSM-5 catalytic performance evaluated in the selective oxidation of styrene to benzaldehyde using TBHP. J Porous Mater 23(3):741–752. https://doi.org/10.1007/s10934-016-0129-8
51. Bai P, Wu P, Xing W, Liu D, Zhao L, Wang Y, Zhao XS (2015) Synthesis and catalytic properties of ZSM-5 zeolite with hierarchical pores prepared in the presence of n-hexyltrimethylammonium bromide. J Mater Chem A 3(36):18586–18597. https://doi.org/10.1039/c5ta05350a
52. Narayanan S, Vijaya JJ, Sivasanker S, Yang S, Kennedy LJ (2014) Hierarchical ZSM-5 catalyst synthesized by a Triton X-100 assisted hydrothermal method. Chin J Catal 35(11):1892–1899. https://doi.org/10.1016/s1872-2067(14)60177-7
53. Noor P, Khanmohammadi M, Roozbehani B, Yaripour F, Bagheri GA (2018) Introduction of table sugar as a soft second template in ZSM-5 nanocatalyst and its effect on product distribution and catalyst lifetime in methanol to gasoline conversion. J Energy Chem 27(2):582–590. https://doi.org/10.1016/j.jechem.2017.10.031
54. Brião GV, Jahn SL, Foletto EL, Dotto GL (2017) Adsorption of crystal violet dye onto a mesoporous ZSM-5 zeolite synthetized using chitin as template. J Colloid Interface Sci 508:313–322. https://doi.org/10.1016/j.jcis.2017.08.070
55. Tao H, Li C, Ren J, Wang Y, Lu G (2011) Synthesis of mesoporous zeolite single crystals with cheap porogens. J Solid State Chem 184(7):1820–1827. https://doi.org/10.1016/j.jssc.2011.05.023
56. Yin C, Feng L, Ni R, Hu L, Zhao X, Tian D (2014) One-pot synthesis of hierarchically nanoporous ZSM-5 for catalytic cracking. Powder Technol 253:10–13. https://doi.org/10.1016/j.powtec.2013.10.027
57. Ma Y, Hu J, Jia L, Li Z, Kan Q, Wu S (2013) Synthesis, characterization and catalytic activity of a novel mesoporous ZSM-5 zeolite. Mater Res Bull 48(5):1881–1884. https://doi.org/10.1016/j.materresbull.2013.01.014
58. Stavrinou A, Aggelopoulos CA, Tsakiroglou CD (2018) Exploring the adsorption mechanisms of cationic and anionic dyes onto agricultural waste peels of banana, cucumber and potato: adsorption kinetics and equilibrium isotherms as a tool. J Environ Chem Eng 6(6):6958–6970. https://doi.org/10.1016/j.jece.2018.10.063
59. Eltaweil AS, Ali Mohamed H, Abd El-Monaem EM, El-Subruiti GM (2020) Mesoporous magnetic biochar composite for enhanced adsorption of malachite green dye: characterization, adsorption kinetics, thermodynamics and isotherms. Adv Powder Technol 31(3):1253–1263. https://doi.org/10.1016/j.apt.2020.01.005
60. Sartape AS, Mandhare AM, Jadhav VV, Raut PD, Anuse MA, Kolekar SS (2017) Removal of malachite green dye from aqueous solution with adsorption technique using Limonia acidissima (wood apple) shell as low cost adsorbent. Arab J Chem 10:S3229–S3238. https://doi.org/10.1016/j.arabjc.2013.12.019
61. Sharma P, Kaur R, Baskar C, Chung W-J (2010) Removal of methylene blue from aqueous waste using rice husk and rice husk ash. Desalination 259(1–3):249–257. https://doi.org/10.1016/j.desal.2010.03.044
62. Sabarish R, Unnikrishnan G (2018) Novel biopolymer templated hierarchical silicalite-1 as an adsorbent for the removal of rhodamine B. J Mol Liq 272:919–929. https://doi.org/10.1016/j.molliq.2018.10.093
63. Sabarish R, Unnikrishnan G (2018) Polyvinyl alcohol/carboxymethyl cellulose/ZSM-5 zeolite biocomposite membranes for dye adsorption applications. Carbohyd Polym 199:129–140. https://doi.org/10.1016/j.carbpol.2018.06.123
64. Sabarish R, Unnikrishnan G (2018) PVA/PDADMAC/ZSM-5 zeolite hybrid matrix membranes for dye adsorption: fabrication, characterization, adsorption, kinetics and antimicrobial properties. J Environ Chem Eng 6(4):3860–3873. https://doi.org/10.1016/j.jece.2018.05.026
65. Vadivelan V, Kumar KV (2005) Equilibrium, kinetics, mechanism, and process design for the sorption of methylene blue onto rice husk. J Colloid Interface Sci 286(1):90–100. https://doi.org/10.1016/j.jcis.2005.01.007
66. Gong J-L, Zhang Y-L, Jiang Y, Zeng G-M, Cui Z-H, Liu K, Huan S-Y (2015) Continuous adsorption of Pb(II) and methylene blue by engineered graphite oxide coated sand in fixed-bed column. Appl Surf Sci 330:148–157. https://doi.org/10.1016/j.apsusc.2014.11.068
67. Ding Z, Hu X, Zimmerman AR, Gao B (2014) Sorption and cosorption of lead (II) and methylene blue on chemically modified biomass. Biores Technol 167:569–573. https://doi.org/10.1016/j.biortech.2014.06.043
68. Golubeva OY, Pavlova SV (2016) Adsorption of methylene blue from aqueous solutions by synthetic montmorillonites of different compositions. Glass Phys Chem 42(2):207–213. https://doi.org/10.1134/s1087659616020073
69. Acemioglu B (2005) Batch kinetic study of sorption of methylene blue by perlite. Chem Eng J 106(1):73–81. https://doi.org/10.1016/j.cej.2004.10.005
70. Aygün A, Yenisoy-Karakaş S, Duman I (2003) Production of granular activated carbon from fruit stones and nutshells and evaluation of their physical, chemical and adsorption properties. Microporous Mesoporous Mater 66(2–3):189–195. https://doi.org/10.1016/j.micromeso.2003.08.028